Clinical and Experimental Medical Sciences, Vol. 5, 2017, no. 1, 35 - 66 HIKARI Ltd, www.m-hikari.com https://doi.org/10.12988/cems.2017.722

Isomer-Specific Trace-Level Biosensing

Using a Nanopore Transduction Detector

Stephen Winters-Hilt

Biology and Computer Science Department
Connecticut College
270 Mohegan Ave.
New London, CT 06320, USA
&
Meta Logos Inc.
124 White Birch Dr.
Guilford, CT 06437, USA

Copyright © 2017 Stephen Winters-Hilt. This article is distributed under the Creative Commons Attribution License, which permits unrestricted use, distribution, and reproduction in any medium, provided the original work is properly cited.

Abstract

A general method for nanopore transduction detection is described that is isomer-specific and operational at low concentration. Nanopore transduction detection operates by transducing single-molecule states into different channel current blockades in a single channel by use of a specially designed transducer molecule that is captured at that channel, blockading its channel current. A new transducer construction is proposed here where transducers based on inexpensive chimeric LNA/DNA nucleic acids are used that provide a means to perform state tracking for both large and small charge/mass biomolecular complexes. The inexpensive nanopore transduction detector system offers the prospect for high-specificity molecular, molecular feature, and particulate testing, not only in the lab setting, but also in the field setting. High-specificity detection is possible by incorporating the high binding specificity of aptamers and monoclonal antibodies for their binding targets into a nanopore binding-event transduction system. High sensitivity detection is possible by using long-lived LNA/DNA chimeric transducer molecules, described here, that can be observed for long periods of time, even under significant strain, allowing a trade-off to longer sampling windows with smaller, even trace level, concentration of analyte of interest. Significant strains can occur when the biosensing system is driven by laser-tweezer pulsing to ensure a channel modulating transducer molecule, to establish a stochastic carrier wave into the signal analysis as described in previous work. Without long-lived transducers, the method favors shorter observations and an ensemble, or assaying, approach rather than the highly sensitive single-molecule tracking/biosensing approach focused on here. Once a binding event is transduced to an electrical (ionic) current flow measurement, novel channel current cheminformatics and machine learning methods can be used for event classification. A quantification of bound versus unbound reporter molecules detected at the nanopore transduction detector then allows the concentration of the isomer target molecule or particulate to be determined.

Keywords: Isomer assay; Nanopore Detection; Single-Molecule Biophysics

1 Introduction

The nanopore transduction detection (NTD) system, deployed as a biosensor platform (Fig. 1), possesses highly beneficial characteristics from multiple technologies: (i) the specificity of antibody binding, aptamer binding, or nucleic acid annealing; (ii) the sensitivity of an engineered channel modulator to specific environmental change; and (iii) the robustness of the electrophoresis platform in handling biological samples [1-6].

A critical component in the NTD system is the transducer molecule. A NTD transducer is typically a compound molecule that serves to transduce the conformational or binding state of a molecule of interest into different channel current modulations. A NTD transducer can often be constructed by covalently tethering a molecule of interest to a nanopore channel modulator. In previous work, using inexpensive (commoditized) biomolecular components, such as DNA hairpins, as channel-modulators, and antibodies as specific binding moieties (with inexpensive immuno-PCR linkages to DNA), experiments were done to analyze individual antibodies and DNA molecules, their conformations, glycosylations, and their binding properties. It was found that in many applications the DNA-based transducers worked well, but in efforts to extend the methodology to biosensing and glycosylation profiling the DNA modulators often had too short a lifetime until melting. To make matters worse, the DNA-based modulators often had internal conformational freedom of their own that complicated analysis of any linked molecule's conformational changes. Worst of all, sometimes the DNA modulators only modulated when unbound (and the NTD method works best with clearly different modulatory states). Efforts to fix the non-modulatory aspect were partly solved by using a laser-tweezer apparatus to drive distinctive stochastic modulatory blockades in the DNA modulator. This was accomplished by introducing a periodic laser-tweezer 'tugging' on channel-modulator variants that had a biotinylated portion that was bound to a streptavidin-coated magnetic bead (another commoditized component). With modulations 'reawakened', however, the number of types of blockade signal appeared to proliferate significantly, and it

wasn't clear if an automated signal analysis could be implemented as had been done previously [1,7].

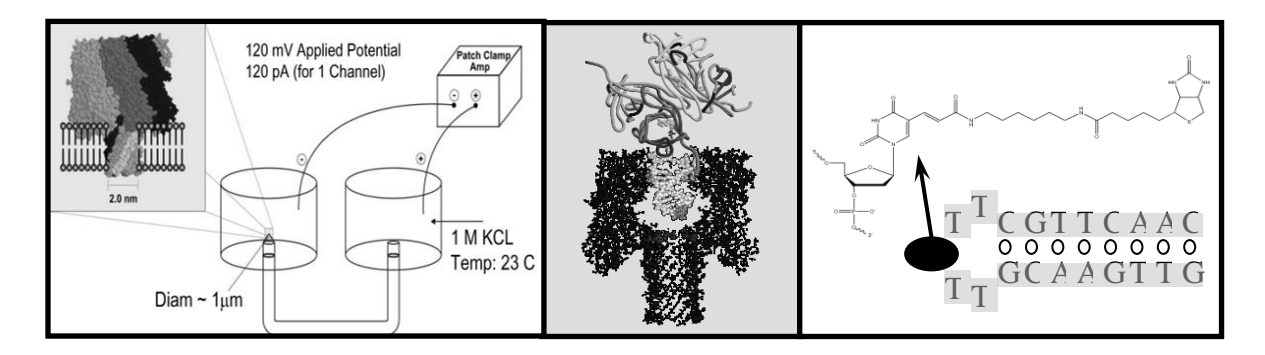


Figure 1. Schematic diagram of the Nanopore Transduction Detector. Left: shows the nanopore detector consists of a single pore in a lipid bilayer which is created by the oligomerization of the staphylococcal alpha-hemolysin toxin in the left chamber, and a patch clamp amplifier capable of measuring pico Ampere channel currents located in the upper right-hand corner. Center: shows a biotinylated DNA hairpin molecule captured in the channel's cis-vestibule, with streptavidin bound to the biotin linkage that is attached to the loop of the DNA hairpin. **Right**: shows the biotinylated DNA hairpin molecule (Bt-8gc). Reprinted with permission [2].

In this paper we show results that support the hypothesis that the new laser-tweezer induced modulator motions are due to duplex DNA twist-dominated toggling (in addition to the previously observed conformation-dominated toggling). A proliferation in modulatory modes beyond shifting and twisting is not seen, however, thus the transducer blockade signal is found to be manageable (computationally) as is. The new understanding suggests that a straightforward, generally-applicable, method for transducer construction is possible with twist-mode dominated state tracking for large charge/mass biomolecules and their binding targets (with long-tether constructions), and configuration-switching dominated state tracking for small charge/mass biomolecules and their binding targets (using short-linkage constructions). General applications of the NTD method are described in what follows for trace-level biosensing, particularly for assaying on isomers.

In NTD binding results and testing results on NTD operation under extreme chaotrope conditions and over a wide range buffer pH [8], it was seen how various molecular strain conditions could lead to isomer splitting on the channel-modulatory molecule often used in transducer designs [8]. For experiments with high levels of chaotrope a clearly identifiable isomer splitting could be seen for the DNA hairpin molecules that were often used as distinctive nanopore blockade modulators. This result not only established further evidence of the ability to resolve isomers on the nanopore detector, but due to the special

channel modulation role of the DNA hairpins examined, this result also clarified the nature of some of the complex channel blockade classes encountered under other strain conditions. The new, less-stable, channel modulations appear to be due to DNA hairpin conformations with variable loop/stem twist. The modulator's isomer 'twist' states typically have one isomer present under low-strain conditions and a second conformation when the molecule is under significant stress, whether due to a high applied potential, higher chaotrope concentration, higher pH, or large charge/mass torque when binding/transducing larger target molecules. The solution to the channel modulators having too short a melting time, and too much internal conformational freedom, turns out to be the same, to use locked nucleic acid (LNA) nucleosides. Chimeric LNA/DNA-based transducers and modulators are described in the results, along with further results on inducing a modulatory blockade by using a laser-tweezer. By establishing a general procedure for NTD transducer design a number of biosensing applications are made possible.

Constructions are thus indicated for using LNA/DNA chimeric three-way Y-transducers and four-way Holliday junction transducers, all locked with LNA's to the extent necessary, to evoke the desired twist-toggling or config-toggling modulations. The binding moiety of the transducer is typically antibody, aptamer, or annealing based. If working with aptamers or annealing, the entire transducer molecule could derive from nucleic acids. The more complex aptamer transducers are particularly relevant when considering therapeutic use of aptamer methods. Aptamer-based therapeutics have begun to get FDA approval in two settings (see Sec. 5.2 for further details): (1) dialysis therapy where aptamer-based filters are used to clean a patient's blood of accumulated kidney or liver toxins that are not being cleared due to damage to those organs; and (2) tissue or tumor directed treatments where the aptamer is linked to an antibody (encompassed by the aforementioned quadfunctional case) already known to target and localize to the tissue or tumor of interest. In the Results, long-term stable chimeric LNA/DNA transducers are shown for biotin-streptavidin binding detection. In the Background that follows the nanopore transduction detector is described, along with transducer engineering methods. The transducers used in the results are described in the Methods.

2 Background

2.1 Nanopore Transduction Detection (NTD)

The nanopore transduction detection (NTD) platform [1,2] comprises a single nanometer scale channel that allows a single ionic current flow across a membrane and an engineered, or selected, channel blockading molecule. The channel blockading molecule is engineered or selected such that it provides a current modulating blockade in the detector channel when drawn into the channel. The channel is chosen such that it has inner diameter at the scale of that molecule or one of its molecular-complexes. For most biomolecular analysis implementations this leads to a choice of channel that has inner diameter in the range

0.1-10 *nanometers* (see Fig. 1). Given the channel's size it is referred to as a nanopore in what follows.

In order to have a *capture* state in the channel with a *single* molecule, a nanopore is needed. In order to establish a coherent capture-signal exhibiting non-trivial stationary signal statistics the nanopore's limiting inner diameter typically needs to be sized at approximately 1.5nm for duplex DNA channel modulators (precisely what is found for the alpha-hemolysin channel). The modulating-blockader is captured at the channel for the time-interval of interest by electrophoretic means.

The NTD molecule providing the modulating blockade in what follows has a second functionality, to specifically bind to some target of interest such that its blockade modulation is discernibly different according to binding state (see the DNA annealing examples in [3] and [4]). Thus, the NTD modulators are engineered to be bifunctional in that one end is meant to modulate the channel current, while the other end is engineered to have different states according to the event detection, or event-reporting, of interest. Examples include extra-channel ends linked to binding moieties such as antibodies or aptamers. Examples also with cleaved/uncleaved 'reporter transducer' molecules extra-channel-exposed ends, with cleavage by UV or enzymatic means [1]. By using pattern recognition to process the channel current blockade modulations, and thereby track the molecular states, a biosensor is thereby enabled.

The weaknesses of the standard ensemble-based binding analysis methods are directly addressed with a single-molecule approach. The role of conformational change during binding, in particular, can be directly explored in this setting. This approach also offers advantages over other translation-based nanopore detection approaches since the transduction-based apparatus introduces two strong mechanisms for boosting sensitivity on single-molecule observation: (i) engineered sensitivity in the transduction molecule; and (ii) machine learning based signal stabilization and highly sensitive state resolution. NTD used in conjunction with recently developed pattern recognition informed sampling capabilities greatly extends the usage of the single-channel apparatus [5] (including learning the avoidance of blockades associated with channel failure, when contaminants necessitate; and nanomanipulation, where we have a single-molecule under active control in a nanofluidics-controlled environment).

With the NTD apparatus the observation is not in the optical realm, like with the microscope, but in the molecular-state classification realm. NTD, thus, provides a technology for characterization of transient complexes. The nanopore detection method uses the stochastic carrier wave signal processing methods developed and described in prior work [1,2], and comprises machine learning methods for pattern recognition that can be implemented on a distributed network of computers for real-time experimental feedback and sampling control [5].

In assaying applications the nanopore detector offers two types of analysis: (1) direct glycoform assaying according to blockade modulation produced directly by the analyte interacting with the nanopore detector, which works on negatively charged glycosylation and glycation profiling best; and (2) indirect isomer assaying by means of surface feature measurements using a specifically binding intermediary, such as with the antibody used in HbA1c testing. A mixture of the direct and indirect assaying methods may be necessary for complex problems of interest.

One of the most challenging nanopore assaying applications is for discriminating between isomers, approximately mass equivalent molecular variants, or aptamers [1,7-11]. Other nanopore-based efforts include DNA sequencing applications, and nanopore device physics studies in general, including with channels other than alpha-hemolysin [12-27].

2.2 Aptamers and their applicability to isomer resolution

Aptamers are nucleic acids with high specificity and high affinity for a target molecule, the properties found to be so useful in monoclonal antibody (mAb) diagnostics and biosensing applications. Aptamer selection is done by a rapid artificial evolutionary process known as SELEX [9]. Nanopore-directed (NADIR) SELEX offers a means to accelerate the SELEX process and arrive at improved outcome, where the standard aptamer sequence library has the constraint that a portion of the sequence self-assemble (anneal) such that it provides an interface with a nanopore detector to provide a modulatory blockade and thereby introduce a 'stochastic carrier wave' (SCW) into the design/detection process [1, 10]. Subject to the SCW constraint the bifunctional aptamer construct already satisfies the criteria to be a nanopore transduction reporter or event 'transducer' [11] (see Fig.'s 2 & 3). If the transducer has a magnetic bead attachment 'arm', then we are now talking about a trifunctional molecule, thus the Y-shaped DNA molecule in many of the discussions that follow. Aptamer design can be quite complicated in some settings, however, such as when the binding target of interest involves large molecular features (for some air or water pollutants), large cell-surface features, heavy metal chelation binding, or because the aptamer transducer is inherently more complex with multiple binding moieties or functionalities, such as with linked double-aptamer constructs and dual aptamer/antibody binding moieties. For the tissue-targeted antibody/aptamer quadfunctional transducer arrangements a 4-way, Holliday-junction, type of DNA molecule could be used (see Disc. For details), or a linkage via more complicated EDC linker technology [10]. The NADIR augmented SELEX procedure is even more advantageous in such settings.

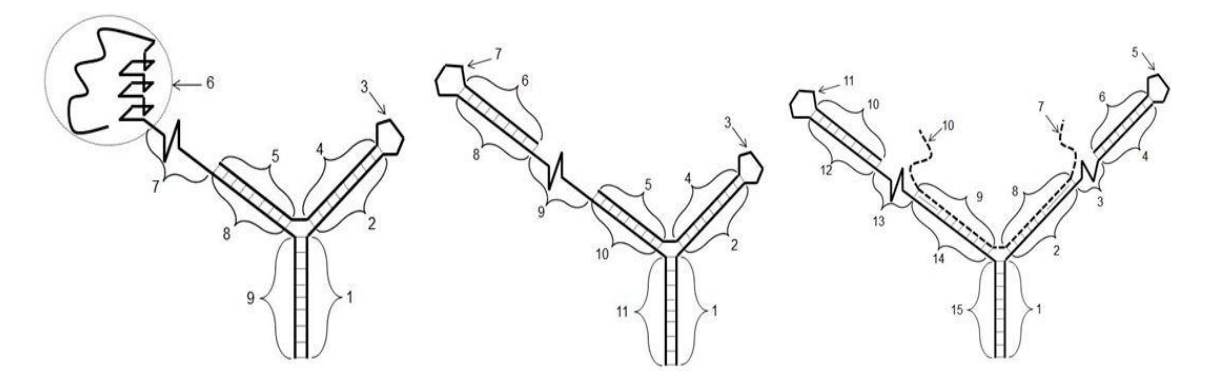


Figure 2. Left. Y-transducer for high-specificity aptamer binding detection. Center and Right: Y-transducers for testing hypothesized miRNA binding sites and/or miRNA interactions with a known miRNA binding site. The Y-transducer is meant to have a high-specificity aptamer attached by a single stranded, possibly abasic (non-base-pairing), nucleic acid linker, region 7, to an aptamer in region 6. The sketch of the aptamer in region 6 is meant to suggest the 3D conformational aspect of the aptamer, where stacking of G-quadruplexes is a common, but not necessary, feature of aptamers.

In Fig. 2, the Y-transducer is comprised of two, possibly RNA/DNA chimeric, nucleic acids, where the first single stranded nucleic acid is indicated by regions 1-5 and the second nucleic acid is indicated by regions 6-9. The paired regions {1,9}, {2,4}, and {5,8} are meant to be complements of one another (with standard Watson-Crick base-pairing), and designed such that the annealed Y-transducer molecule is meant to be dominated by one folding conformation (as shown). The region 3 is a loop, typically 4 dT in size, that is designed to be too large for entry and capture in the alpha-hemolysin channel, such that the annealed Y-transducer only has one orientation of capture in the nanopore detector. The base region, comprising regions {1,9}, is designed to form a duplex nucleic acid that produces a toggling blockade when captured in a nanopore detector. The typical length of the base-paired regions is usually 8-10 base-pairs.

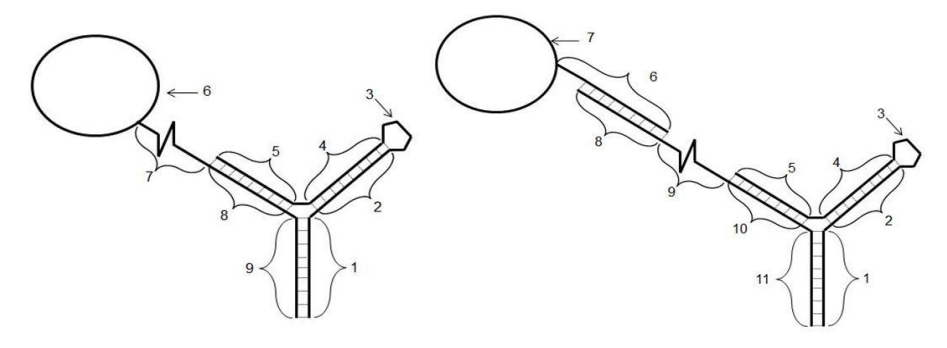


Figure 3. Y-transducer for high-specificity antibody binding detection.

2.3 Engineering NTD Transducer/Reporter Molecules [42]

In previous NTD work the presence of a specific five base length nucleic acid was ascertained [3], and an eight base sequence of DNA was ascertained with very high specificity with the introduction of urea as a chaotrope [2]. In the latter work, the DNA annealing based detection was performed with a Y-shaped DNA transduction molecule engineered to have a DNA hairpin with complementary overhang as binding partner. Figure 4 shows the binding results as a collection of single-molecule sample events.

Eight and nine base-pair DNA hairpins have been used as channel modulators previously [2], where the modulator had a covalently attached binding moiety (biotin or linked antibody) that was tracked as to its binding state (by measuring the channel modulation exhibited by the channel-captured DNA hairpin ends, see Fig. 1 for the biotin-streptavidin binding study). Further developments along these lines without a linker arrangement, where a more commoditized methodology is used, led to the DNA 'Y-transducer' platform (see Fig.s 2 & 3). The Y-transducer has also been used in experiments showing DNA-DNA annealing on 5-9 base nucleic acids, and in transducing DNA-protein (HIV integrase, TBP) binding events [6]. A limitation in all of these efforts was that the critical length of duplex nucleic acid needed for modulation, ranged from 8 to 10 base-pairs for the alpha-hemolysin nanopore platform that was being used. (Reasons for the alpha-hemolysin platform being used can be found in [1, 15].) The short duplex lengths meant that the transducer/reporter molecule could only be observed for seconds or minutes before its Watson-Crick base-pairing dissociates and the duplex nucleic acid becomes single-stranded, i.e. it 'melts', forcing the NTD to favor a rapid-sampling ensemble detection mode on the transducer/reporter molecules [5], and less in the single-molecule event-tracking mode that might otherwise be optimal for some applications, like those focused on here.

Often the *bound* state of the transducer/reporter molecule was found to transduce to a fixed-level blockade (i.e., the transducer provides distinctive channel modulation when unbound, but not so distinctive fixed-level channel blockades when bound [1]). It is necessary to have *both* the bound and unbound transducers with distinctive channel modulations in order to have automated high-precision state identification and tracking (and allow for multiplex assaying). The switch to a fixed-level blockade might be due to the electrophoretic force on the the large bound complex forcing the channel-captured end to reside in one blockade state. This was explored in experiments where a streptavidin-coated magnetic bead was attached to biotinylated DNA hairpins [7]. Once a streptavidin coated magnetic bead was attached to the biotinylated hairpins, a laser-tweezer tugging allowed distinctive channel modulation to result (see Fig. 4). It was found in more recent work that the induced blockade modulations occurred in two types (this is seen to occur in [8] for chaotrope induced, see Fig. 5; and in [7], see Fig. 4, for early laser-tweezer induced results. Further laser tweezer results showing the different,

overlapping, modes are shown in the Results, where the experiments are done with a DNA-hairpin transducer.

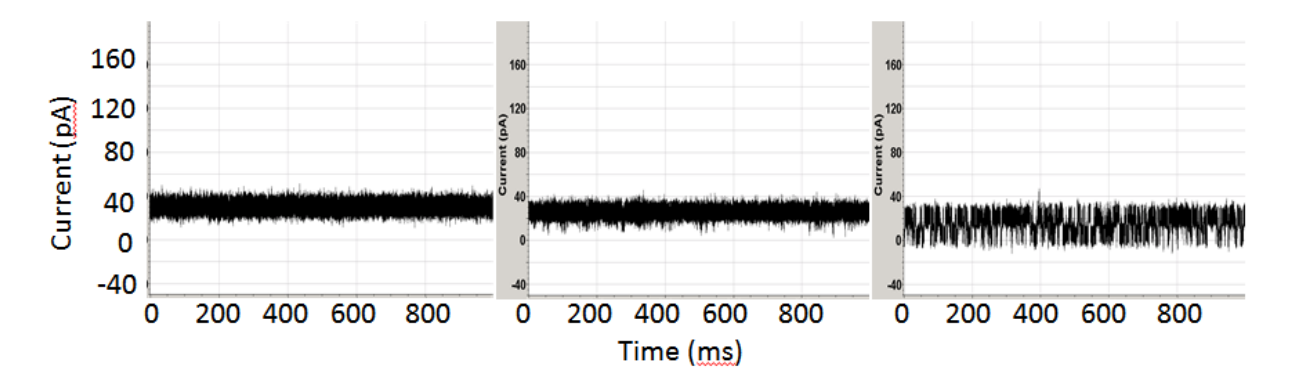


Figure 4. A (Left) Channel current blockade signal where the blockade is produced by 9GC DNA hairpin with 20 bp stem [4]. (Center) Channel current blockade signal where the blockade is produced by 9GC 20 bp stem with magnetic bead attached. (Right) Channel current blockade signal where the blockade is produced by c9GC 20 bp stem with magnetic bead attached and driven by a laser beam chopped at 4 Hz. Each graph shows the level of current in picoamps over time in milliseconds. Reprinted with permission [4].

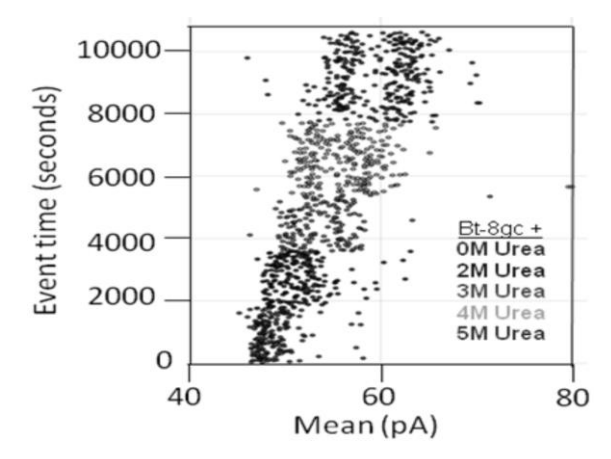


Figure 5. Bt-8gc transducer blockade signals in the presence of high urea concentrations. Sufficiently strong Urea concentration (5M) results in racemization of the two loop capture-variants, while weaker urea (<2M) does not. The results show Bt-8gc measurements at 30 minute intervals (1800 s on vertical axis) with urea concentration 0, 2, and 3M, 45 minutes at 4M, and 60 minutes at 5 M, with signal blockade mean on the x-axis. The results are consistent with the two-state loop hypothesis, and consistent with the observation of such in Fig. 1 (see [2]) that were not due to high urea content but due to high strain due to mass and charge effects. Reprinted with permission [8].

Two twist conformations in the hairpin loop and stem duplex conformation (such as B, B*, or A/B conformation duplex DNA), have been suspected from results on the DNA hairpins under a variety of strain conditions, such as high voltage settings (greater than 180mV, where 120mV was the typical experimental setting). So, it is not unexpected that two types of DNA hairpin channel blockade modes should appear in the laser-tweezer experiments. The modes are thought to be of two types because there are two types of general molecular motion: rigid-body configuration changing, or 'toggling'; and internal configuration changing, or 'twisting'. Although the resulting toggle/twist mode signal analysis is more complicated this is actually a highly favorable result. This is because a bound transducer that can provide a modulatory state by use of a bead attachment with laser excitation, even with two types of modulation signal resulting, is still a very manageable situation. Thus, the stochastic carrier wave analysis [1] can proceed as before, only with the additional training data needed to 'learn' the more complicated background 'carrier wave' signal. This is good news because the new mode types don't appear to proliferate beyond the new twist modes seen. The transducer problem thereby remains tractable with laser-tweezer generalized (ubiquitous) transducer design. There is also the possibility to turn the twist mode type of internal signaling to our advantage in specialized transducer designs, as will be seen in the following.

The Y-shaped DNA transduction molecule is a versatile construct in and of itself to test for as an intermediate annealed complex, as evidenced in single nucleotide polymorphism SNP detection efforts [4]. Highly accurate SNP detection with the Y-shaped DNA transduction molecule was possible in [4] by designing the Y-transducer to anneal to nucleic acid target sequence such that the SNP variant occurs in the Y-nexus region, giving rise to a clear difference in the annealed Y-transducer's channel modulation. The NTD method provided a means to perform SNP variant detection to very high accuracy, and will likely be improved further when using the higher specificity LNA form of the transducers indicated by the LNA improvements seen in the Results.

3 Methods

3.1 Nanopore Detector Experiments

Each experiment is conducted using one alpha-hemolysin channel inserted into a diphytanoyl-phosphatidylcholine/hexadecane bilayer across a 20-25 micron-diameter horizontal Teflon aperture. The alpha-hemolysin pore has a 2.0 nm widthat its outer, vestibular, opening, allowing a dsDNA molecule to be captured. The effective diameter of the bilayer ranges mainly between 5-25 μm. This value has some fluctuation depending on the condition of the aperture, which station is used, and the bilayer applied on a day to day basis. Seventy microliter chambers on either side of the bilayer contain 1.0 M KCl buffered at pH 8.0 (10 mM HEPES/KOH). Voltage is applied across the bilayer between Ag-AgCl electrodes. DNA control probes are typically added to the *cis* chamber at 10-20 nM

final concentration. All experiments are maintained at room temperature (23 ± 0.1 °C), using a Peltier device. Details on controlling the nanopore noise sources and aperture construction are given in the Suppl. Sec. S.1

3.2 DNA probes

Biotinylated DNA probes (from IDT DNA, purification by PAGE)

8GC-BiodT: 5'- GTCGAACGTT/iBiodT/TTCGTTCGAC -3' 9GC-BiodT: 5'- GTTCGAACGTT/iBiodT/TTCGTTCGAAC -3'

Biotinylated LNA/DNA Chimeric probes (from Exigon, purification by HPLC)

8GC-BiodT: 5'- +G+TCGAA+C+GTT/iBiodT/TT+CGT+T+CG+AC -3'. The LNA version of 8GC-Bt has 8 LNA bases shown preceded by '+', 12 DNA bases, and 1 biotin dT base.

9GC-BiodT: 5'- +G+CTTGAA+C+GT/iBiodT/TT+CGTT+CAA+GC -3'. The LNA version of 9GC-Bt stem does not have the same sequence as the DNA-based 9GC, and has only a 3dT loop aside from the modified dT with biotin attachment, and has 7 LNA bases shown preceded by '+', 14 DNA bases, and 1 biotin dT base.

<u>Laser Trapping probes (from IDT DNA, purification by HPLC)</u>

The 20bp hairpin with 4dT loop:

9GC-ext: 5'- GTTCGAACGGGTGAGGCGCTT

TTGCGCCCTCACCCGTTCGAAC -3'

The 20bp hairpin with 5dT loop, where the central loop dT was modified to have a linker to biotin:

9GC-BiodT-ext: 5'-

GTTCGAACGGGTGAGGGCGCTT/iBiodT/TTGCGCCCTCACCCGTTCGAACC-3'

3.3 Conjugation to Magnetic Beads

The streptavidin-coated magnetic bead diameters were approximately 1 micron and the mass about 1 pg. Some of the bead preparations involved use of BSA buffer, which required tolerance of BSA at the nanopore detector. This was separately confirmed for the concentrations of interest, up to the level of 8mg/mL BSA, in preliminary tests for bead usage.

3.4 Laser Setup

Laser illumination provided by a Coherent Radius 635-25. Output power before fiber optic was 25mW at a wavelength of 635 nm. The beam was chopped at 4Hz. During laser excitation studies the Faraday cage was removed. Significant 60 Hz wall-power noise was not seen with case removed when there was no laser illumination, but with cage removed and under laser illumination 60Hz line noise could clearly be seen. The 60 Hz line noise was, thus, picked up at the laser's power supply and transmitted via the laser excitation process into the detector environment

as a separate modulatory source. After fiber optic, approximately 5-10mW illumination focused to an approximate 1mm illumination diameter was produced at the nanopore detector's aperture.

3.5 Use of chaotropes to improve signal resolution

In the nucleic acid annealing studies on the NTD platform described in [2], the highly beneficial role of chaotropes for robust nucleic acid annealing studies on the NTD platform was revealed. The ability of the NTD apparatus to tolerate chaotrope concentration, up to 5M urea, was demonstrated in [8], where the DNA hairpin control molecules demonstrated a manageable amount of isomer variation even at 5M urea (see Fig. 5). In the study in [28] it was shown how urea could destabilize the alpha-hemolysin channel, so the results in [8] were somewhat surprising. It is hypothesized that the dsDNA hairpin transducer molecules used help to maintain the alpha hemolysin channel, possibly by sterically hindering vestibule/channel collapse.

3.6 Managing common interference agents and antibody interference & transduction capability

The electrophoretic mechanism of the NTD detector operation provides a huge advantage when dealing with possible contaminants. Electrophoresis is used to drive strong negative charges to the nanopore detector. Since nucleic acids are strongly negatively charged they will be separated and driven to the detector, along with certain proteins and other molecules that have a low pI. Most proteins with low pI are found to have very little interaction with the nanopore channel, however, the main exception being antibodies [29]. Consider the common level of interference agents used for medical testing applications (see Table 1). Actual levels of interference agents seen in (healthy) human blood samples are far lower (see Table 2). As a test situation, consider working with a 1uL sample (such as with a pinprick sample) that contains high levels of common interference agents from blood, etc. Table 3 shows the very high contaminant levels that have been tested on the NTD with very low concentrations of reporter molecule, and the reporter molecules are easily discerned (see Results for further details). Most interference agents pose little channel interaction. The main exception involves proteins or protein fragments involving antibodies. A single monoclonal antibody (mAb) is found to produce a variety of distinct channel modulation signals types. Some mAb blockades produce a very clean toggling between two levels, like that of the 9GC DNA hairpin control molecule. The modulatory signals are easily discerned from each other, however, especially with increased observation time as needed (and can be incorporated into the auto-eject tuning, see PRI background information for further details). Aside from being an interference agent, antibodies can be a NTD transducer themselves since their modulatory blockade signals are observed to change upon introduction of antigen (to produce distinctively new signals only associated with introduction of the antigen). The problem with using an antibody directly as a transducer is that the antibody produces multiple blockade signal types just by itself. This weakness for direct mAb use as a NTD transducer (they can still

be linked indirectly as in [7]) is because the antibody is a glycoprotein that has numerous heterogeneous glycosylations and glycations, with many molecular side-groups that might be captured by the nanopore detector to produce modulatory blockades. If the purpose is to study the post-translational modifications (PTMs) themselves, a glyco-profile in other words, then the numerous signal types seen are precisely the information desired. A more complete analysis of antibody blockades on the nanopore detector is given in [29, 30].

Bilirubin:	10mg/dL = 0.10mg/mL
Cholesterol:	800 mg/dL = 8.00 mg/mL
Hemoglobin:	250 mg/dL = 2.50 mg/mL
Triglyceride:	500 mg/dL = 5 mg/mL

Table 1. Common level of interference agents used to demonstrate robust medical testing applications. Reprinted with permission [11].

Bilirubin	5mg/L (10uM)
Cholesterol (healthy)	< 2mg/mL (5mM)
Hemoglobin in plasma	2mg/dL = 0.02mg/mL (300nM)
Hemoglobin in whole blood	150mg/mL(2.5mM)
Triglyceride	1g/L (1mM)
Serum DNA (no cell ruptures)	1-200ng/ml
Albumin	35-50 g/L (600uM)
Immunoglobulin G (IgG)	15mg/mL (at 160kDa → 93.75nmol/mL)
Urea	15 mg/dL (3mM)
Glucose (fasting)	100 mg/dL (5mM)

Table 2. Actual levels of interference agents seen in (healthy) human blood samples. Reprinted with permission [11].

Cholesterol (healthy)	8 mg/mL > 2 mg/mL
Hemoglobin	4mg/mL > 2.5mg/mL
Immunoglobulin G (IgG)	30 mg/mL > 15 mg/mL
Urea	> 5M >> 3mM
Glucose	>> 50mM > 5mM

Table 3. Contaminant levels that have been tested where reporter molecules are easily discerned. Reprinted with permission [11].

3.7 Data acquisition and Signal Processing

Data is acquired and processed in two ways depending on the experimental objectives: (i) current filtered at 50 kHz bandwidth using an analog low pass Bessel filter and recorded at 20 µs intervals using an Axopatch 200B amplifier (Axon Instruments, Foster City, CA) coupled to an Axon Digidata 1200 digitizer, where, semi-automated analysis of transition level blockades, current, and duration were performed using Clampex. (ii) using LabView based experimental automation. In this case, ionic current was also acquired using an Axopatch 200B patch clamp amplifier, but it was then recorded using a NI-MIO-16E-4 National Instruments data acquisition card. In the LabView format, data was low-pass filtered by the amplifier unit at 50 kHz, and recorded at 20 µs intervals. Signal acquisition from the 20 µs sample stream was done using a Finite State Automaton (FSA) [1, 31]. Further details on the Signal Processing are given in Suppl. Sec. S.2.

3.8 Channel Current Cheminformatics (CCC)

In the NTD platform, sensitivity increases with observation time in contrast to translocation technologies where the observation window is limited to the translocation time. Part of the sensitivity and versatility of the NTD platform derives from the ability to couple real-time adaptive signal processing algorithms to the complex blockade current signals generated by the captured transducer molecule [1].

3.9 Pattern Recognition Informed (PRI) Sampling

For experiments with PRI sampling, a capture signal generated with the nanopore apparatus is filtered and amplified before it is sent through the DAQ. In the pattern recognition feedback loop, the first 200 ms detected after drop from baseline are sent via TCP-IP protocol to the HMM software, which generates a profile for each signal sent. The HMM-generated profile is processed using the previously trained SVM classifier to determine whether the signal is acceptable. If the signal is acceptable, the molecule is not ejected from the channel by the amplifier. If not acceptable, the amplifier briefly reverses the polarity to eject the molecule from the channel.

The channel characteristics are very stable when exposed to interference agents. Some agents if present with sufficiently high concentration, however, can damage the bilayer. Albumin is an example of such and it is the main protein found in blood samples. Albumin can intercalate into the bilayer, causing bilayer disruption, compromising the entire experiment. There are a variety of buffer modifications that can be introduced that are protective of the bilayer, including blocking the albumin intercalation. In doing so, however, new interference molecules are introduced that can damage the channel. The channel destruction problem (caused by trying to protect the bilayer) is found to only be a problem if the protocol is non-

responsive, e.g. if the blockade is not recognized as a 'bad' blockade and ejected promptly (if not ejected promptly the molecule gets 'stuck'). What is needed, and what is used here, is an auto-eject cycle for whatever minimal observation time to minimize channel blockade time regardless (we will see this feature used in the Results that follow). What is also needed is good and bad signal recognition. Generally any signal that is modulating is good, so if all signals are rejected if non-modulatory in their first 0.5 seconds this is a pretty good operational setting. The PRI sampling can thus be employed, indirectly, to provide channel protection and maintain operational status for prolonged periods.

4 Results

4.1 Long-lived chimeric LNA/DNA transducers

Experiments are done with a biotinylated LNA/DNA chimeric 9bp hairpin (LNA 9GC-Bt) in pH 9 that has been linked to a streptavidin-coated magnetic bead. LNA 9GC-Bt with streptavidin bound shows a new mode of toggle (Fig. 6 & 7). Possible twist mode switching is found for the large mass binding case here as with high pH (>9 pH), high voltage (>200mV), and under laser-tweezer inducement to follow. In Fig. 7, the molecule appears captured in one twist/configuration, then shift to the other twist may briefly occur, from which a configuration toggling commences. The configuration toggle appears to involve blockade positions favored by neither of the twist conformations. The captured molecular excitations typically start, as it does here, in what is thought to be a DNA-hairpin twist-modulation mode (a direct consequence of conservation of angular momentum and the large mass streptavidin attachment), eventually this settles into a configuration-toggle mode -- where one configuration is sufficiently deep that DNA terminus fraying and extending can sometimes be observed, as in previous studies [31, 32].

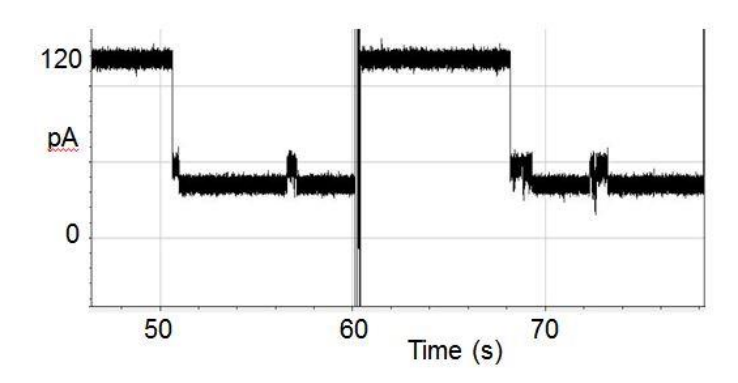


Figure 6. LNA 9GC-Bt blockade signals at 500pM concentration in the detector well at pH9. Auto-eject time is set at 10s. The LNA 9GC-Bt blockades have a faster 'toggle' than LNA 9GC-Bt at pH8.

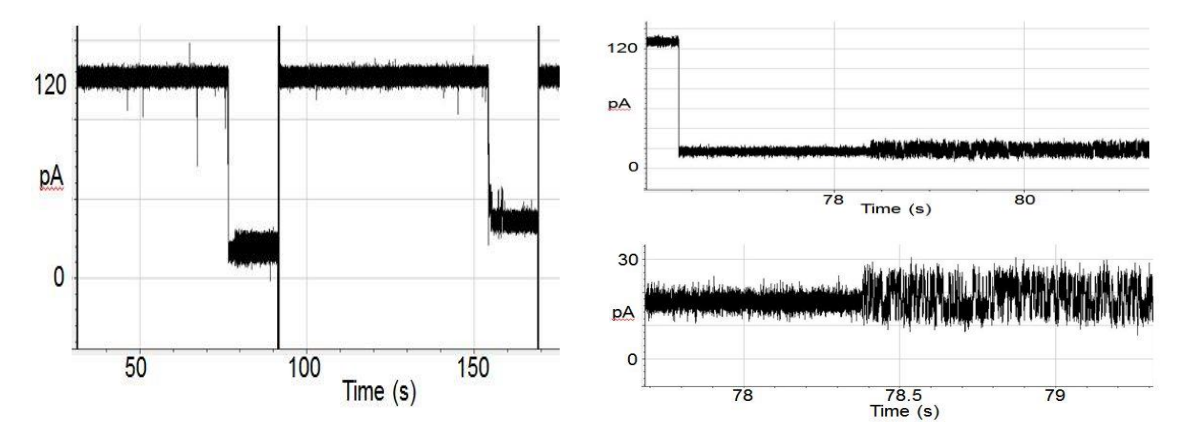


Figure 7. Left: LNA 9GC-Bt blockade signals at 250pM concentration in the detector well at pH9, with streptavidin added 1:1, taken in the first 10 min. Auto-eject time is set at 10s. Bound blockade signals are now seen (the one with the lower blockade level on the left). The bound LNA 9GC-Bt blockades now occasionally have a 'toggle' or switch to a toggle mode (the bound blockade on the left shows a transition to toggle 2s into the bound blockade). Right Top: Enlarged view of bound LNA 9GC-BT blockade. Right Bottom: Further enlarged view of bound LNA 9GC-BT blockade.

4.2 Twist modes

Experiments with biotinylated DNA20bp hairpins [11] (9GC-ext) (Suppl. Sec. S.4, Suppl. Fig. 1) that are linked to streptavidin-coated magnetic beads in pH 8 are shown next (Suppl. Fig. 2 and Fig. 8). The transducer DNA hairpin has stem length twenty base-pairs (20bp) and loop size 5 dT, with the central thymidine modified with a linker to biotin. The hairpin in this form is referred to as 9GC-ext because it is a 20bp extension of the biotinylated 9GC control molecule that has a 9bp stem. The hairpin is then mixed with a solution of magnetic beads that have a streptavidin coating, leading to complexes of magnetic beads attached to a DNA hairpin channel modulator (9GC-ext-mag) by way of a streptavidin-biotin linkage (with early captures like Suppl. Fig. 1). The mass of the magnetic bead is substantially greater than the hairpin, such that upon capture the likelihood of twist mode being excited is even greater, e.g., a huge angular momentum impulse would occur on capture. As the experiment proceeds, however, the twist modulating captures increase in likelihood apparently due to more beads becoming more bound with hairpin and thus more mass and charge, thus greater angular momentum impulse on capture. In Fig. 7 we see an example of hypothesized bound state spontaneously being excited into a modulating blockade signal. If the blockade signal for the bound transducer had such modulations for a large portion of observed blockade time, this would be almost as good as a fully modulatory bound state, and strong SCW-type state resolution could still be done. In general, however, bound transducers appear to become 'stuck' in a fixed blockade level, so a procedure to have bound (and unbound) transducers modulate is still needed, and results along these lines are described next.

It was shown in [7] that laser-tweezer pulsing could induce a transition from a fixed-level to a toggling blockade on biotinylated 20bp DNA hairpins. It was not clear at that time however, that there was both spatial configuration switching and twist configuration switching, because the latter switching hadn't been seen before. The existence of two loop/stem twist configurations began to become apparent, however, as experiments began to explore a variety of strain conditions, such as high urea (such as 2-5M concentration of chaotrope, see Fig. 5) [8], higher than the 120 mV applied potential (such as 150-180 mV), higher pH (9 or greater), or in the presence of large bound charge/mass objects (e.g., streptavidin, streptavidin-bead, antibody, or large-antigen attachment).

In Fig 8 we see a channel blockade due to 9GC-ext-mag in the presence of laser-tweezer pulsing (using a chopped laser beam with an off-target edge-illumination intensity gradient). The upper 'twist-level' is briefly seen initially as before (the 42pA level), followed by a switch to the lower-level twist blockade that has its own, laser-induced, toggle, before sticking at the lower twist state's lower blockade level at the end of the trace (the sticking could be due to the magnetic bead attaching other biotinylated hairpins with increase in charge and overall electrophoretic driving force). Fig 8 Right is an enlarged view of the lower twist state's laser induced toggle as it finally becomes 'stuck' at one level. Note the clear 60 Hz line noise evident in the enlarged view. This noise is not present in 9GC-ext-mag blockades without laser illumination (and without cage), so the 60Hz line noise is being coupled into the measurement via the laser beam having 60Hz noise, not via the unshielded surroundings. The laser was found to induce the most notable switching in the lower-level twist state when chopped at 4Hz.

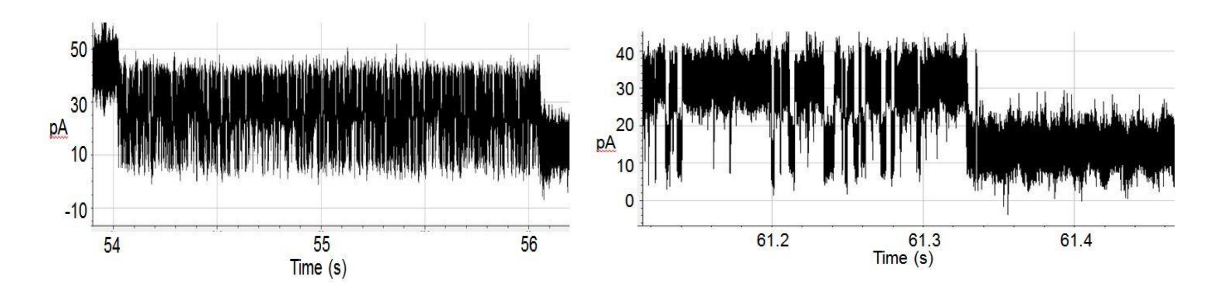


Figure 8. Left: A 9GC-ext-mag blockade signal with Laser-Tweezer modulation (no cage) [11]. The upper-level twist state is now at ~45pA, and the lower-level twist state itself toggles between 30pA and 15pA (with fraying 'spikes' to 0pA as seen in other hairpin studies [31,32]). Right: Enlarged view of lower-level twist toggling, then sticking at its lower level (note the 60Hz noise is from the laser; without laser, but no cage, there is no 60Hz noise). The beam chopper frequency is 4Hz, but the 'awakened' stochastic modulation is non-periodic.

Clearly the twist toggle adds complication on top of the spatial configuration-toggle and this impacts the design of the transducers. Use of LNAs to lock the twist configuration is expected to eliminate the loop-stem twist toggle complication, but it's not as if the signal processing can't manage the two-toggle mode signal. In fact, this and results from similar experiments indicate that there is not further modal proliferation beyond the twist mode addition to the (rigid body) channel capture orientation 'toggle' mode. So, the main purpose in tuning the LNA content in the LNA/DNA chimeras is to select the most effective transmission of binding event to the channel modulator, where most effective could be via twist mode transmission with large-mass long-tether (long DNA arm), while most effective may indicate very rigid (lots of LNA) with low-mass short-arm tethering linkages.

The laser-tweezer excitation clarified the new twist modes, by effectively allowing them to be turned on and off. Returning to the spontaneous added twist modes occasionally seen with 9GC-Bt/streptavidin (Fig. 7) we expect even more notable twist mode to be spontaneously induced with the larger 9GC-ext-mag molecule, especially upon initial capture, due to its larger mass attachment to the nucleic acid modulator portion. This is found to be the case and, in turn, allows new understanding of the complex blockades previously observed when the channel transducer was examined with magnetic bead attached, but not driven by laser (and fully shielded under Faraday cage). A large amount of twist toggling is associated with 9GC-ext-mag blockades: the extended 20bp DNA hairpins typically lasted ~50-60s, often several minutes, before diffusing away, but in some instances only lasted a few seconds (Fig. 9). In order to understand the signal, imagine that there are two dominant twist configurations for the molecule and two dominant channel-blockading configurations (toggles). When first captured the transducer molecule might reside in a twist configuration that has yet to reside in one of the dominant channel-configuration (toggle) modes. The twist blockade has two forms of blockade associated with the two dominant twists. We see this as two levels of blockade, each with its own noise properties, where one is referred to as the 'lower level' (LL), and the other the 'upper level' (UL). Once a capture has settled down, it is usually describable in terms of twist {LL,UL} blockades and toggle {LL,UL} blockades and their overlap occurrence. Consider Fig. 9 in this regard. It starts in a twist-LL capture and shifts (at about 49.5s) to a twist-LL/toggle-{LL,UL} switching blockade (according to the toggle {UL,LL} mode), which lasts from 49.5s to about 50.3s, when a transition to a twist-UL blockade occurs (non-toggling, from 50.30s to 50.45s). At about 50.45s the blockade returns to a twist-LL/toggle-{LL,UL} switching until 50.80 s when a transition to a twist-LL blockade occurs (non-toggling, from 50.80s to 51.00s). From 51s to the end of the blockade signal it then returns to a twist-LL/toggle-{LL,UL} switching.

Sometimes there is observed a lengthy twist-toggle event that eventually settles down to a fixed-level twist-LL blockade. One such signal is shown in its lengthy toggle portion (Fig. 10) that eventually trails off to the fixed level. An enlarged view of one of the twist-LL blockades from the middle of Fig. 10 Left is shown in Fig. 11. The twist-LL state clearly exhibits the familiar fraying terminus type of

blockade signal observed in other DNA hairpin studies on the alpha-hemolysin nanopore detector [31, 32].

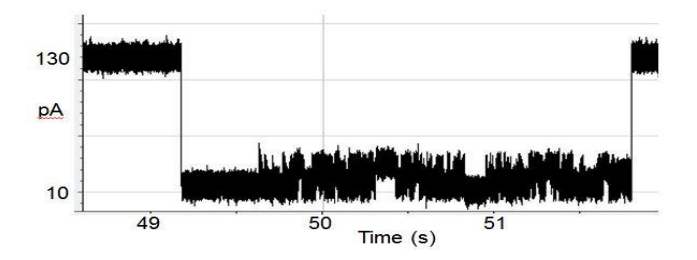


Figure 9. A 2.5s 9GCext_mag blockade with cage, starts at twist-LL then twist-LLtoggle, then twist-UL (which doesn't notably toggle), then twist-LL toggle, then twist-LL briefly stuck in its lower level, then twist-LL toggle.

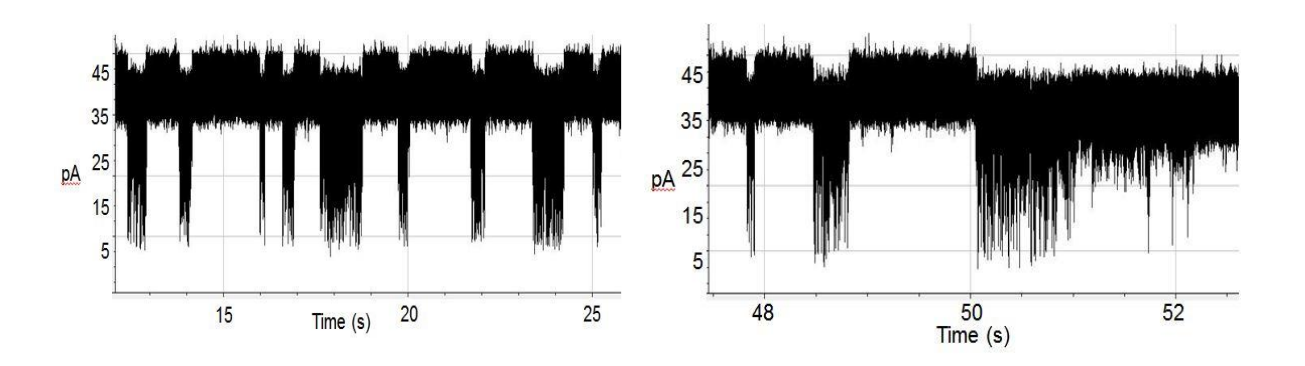


Figure 10. Left: A portion of the lengthy body of a 9GCext_mag blockade signal (with cage), about a tenth of the signal in this mode of toggling is shown. The molecule in the twist-LL state appears to be experiencing fraying-type 'spike' blockades (15sec trace). Right: The end of the twist-toggling part of the 9GCext_mag blockade signal. The final transition is to the twist-LL state, for which the fraying falls off until entirely gone, the blockade then continues in the twist-LL fixed blockade (without 'fraying spikes) for several minutes before ending. As the twist-LL state with frequent fraying events 'settles down' to the twist-LL upper blockade level. Eventually the downward spike fraying events stop entirely. This may be due to the twist-LL having an overall channel-orientation that is slightly pulled out of the channel due to the large magnetic bead attachment, or may simply be due to the molecular excitation damping out, with subsequent less frequent fraying events.

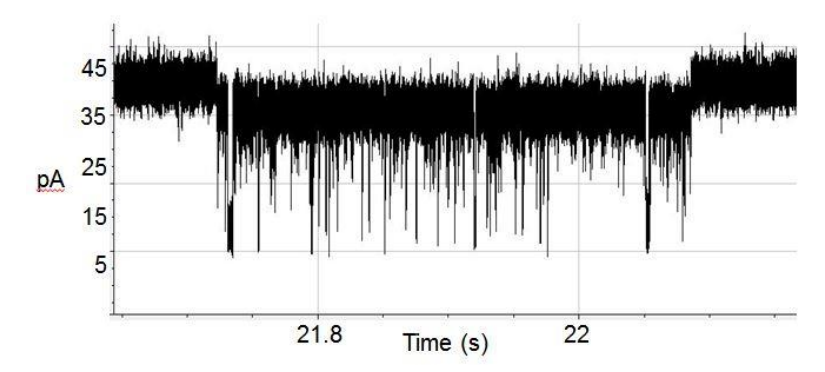


Figure 11. An enlarged view of the 9GCext_mag blockade shown in Fig. 10 Left for one of the twist-LL sections. The twist-LL state clearly exhibits the familiar fraying terminus type of blockade signal observed in other DNA hairpin studies on the alpha-hemolysin nanopore detector [31, 32].

5 Discussion

The discussion that follows focuses on three areas directly pertinent to the conclusion that inexpensive, accessible transducer detection is possible. In Sec. 5.1 it is shown the strong excitation of the DNA hairpin modulators results in two blockade modulation or mode types, one due to bulk-orientation switching by the transducer in the channel, and one due to internal conformational twisting by the dsDNA transducer. In Sec. 5.2 the discussion turns to transducer design issues. Sec. 5.3 briefly describes glycosylation assays and viral nucleic acid assays.

5.1 Two molecular modes – two molecular signal classes

It is shown that nanopore-captured DNA hairpin modulators can exhibit not only spatial/orientation toggling but also torsional/twisting toggling when sufficiently excited. This effect becomes most notable when channel modulations are induced by laser-tweezer pulsing, but has been observed in other high-strain conditions for captured DNA hairpin channel modulators, such as high chaotrope, high pH, high applied voltage, and high mass/charge capture events. The new understanding of the laser-tweezer induced modulations suggests a limit for the induced modulator's signal classes to those already seen and a manageable signal analysis platform can thereby be implemented. In practice a stochastic channel modulator that produces the simplest, non-fixed-level, stationary signal blockade is desired, such that the stochastic carrier wave (SCW) signal processing methods can be employed [1]. The position and twist toggle modes in the modulator together pose a more complex SCW system, but could be managed with sufficient sample observations on modulator during its different states (such as linked to bound or unbound analyte). A related problem with the DNA-based channel modulators has been their short lifetimes until melting. This problem has been eliminated by use of LNAs, where LNAs also serve to reduce twist modes as needed as well, to simplify the SCW basis mentioned above. Since the simpler SCW analysis is not critical, however, the main optimization to be accomplished by 'locking up' the modulator with increased

LNA is effectively a tuning over molecular variants with greater or lesser twist mode event transmission. A general method for transducer construction is thereby suggested with twist-mode dominated state tracking for large charge/mass biomolecular complexes with long duplex DNA tether constructions, and configuration-switching dominated state tracking for small charge/mass biomolecule complexes with short-linkage constructions. Further details on Isomer transducer design and chelator design is given in [42].

5.2 Therapeutics: Complex chelation therapy and molecular therapeutic design and testing

The problem with the DNA transducers that are too easily melted (from duplex nucleic acid to ssDNA), and the internal mode transmission transducers (from one conformation to another – e.g., 'twisting'), is they have too much internal freedom. If it was possible to 'lock-up' some of the internal twist motion, then a stronger hairpin might result, and one less likely to have twist modulations on top of toggle modulations. Such nucleic acid variants are easily implemented by using locked nucleic acid nucleosides (LNAs). LNAs are a nucleic acid analogue where the ribose ring is locked into a highly favorable configuration for Watson-Crick base-pairing. The locking is done by establishing a methylene bridge from the 2'-O atom to the 4'-C atom of the ribose ring. LNA oligonucleotides can be synthesized using standard phosphoamidite chemistry and can be incorporated into chimeras with RNA and DNA. The high affinity of LNA for complementary RNA provides improved specificity and stability. The increased affinity leads to much more stable LNA hairpin and other LNA duplex configurations. This has special significance in the nanopore transduction detector setting where specially designed DNA hairpin and Y-transducer molecules have been identified for use as event transduction molecules, and minor alterations on these transducers for the LNA form (see Methods) can be easily found that will retain the transducer's modulator properties, but now with the long-lived and improved specificity and affinity attributes of LNAs. LNA versions of the biotinylated hairpins studied in [2] are explored in the Results, where the lifetime of the LNA/DNA chimeric transducer molecules in the high-strain capture environment of the nanopore is now on the order of hours instead of minutes.

A Y-transducer for annealing-based detection with no laser-tweezer needed could have a form like in Fig. 12 Left, where the regions with high LNA content are shown in dashed boxes. The LNA at the boundary regions protects the molecule in those regions from terminus fraying, loop opening, or nexus opening. Fig. 13 show a Y-transducer for single molecule studies using twist mode modulations. Nucleic acids can be arranged in other useful geometries than the three-way 'Y' junctions used thus far. Fig. 12 Right shows a 4-way transducer for dual aptamer/antibody tissue-targeting functional aptamer delivery studies, where a modulatory transducer is enabled by laser-tweezer coupling.

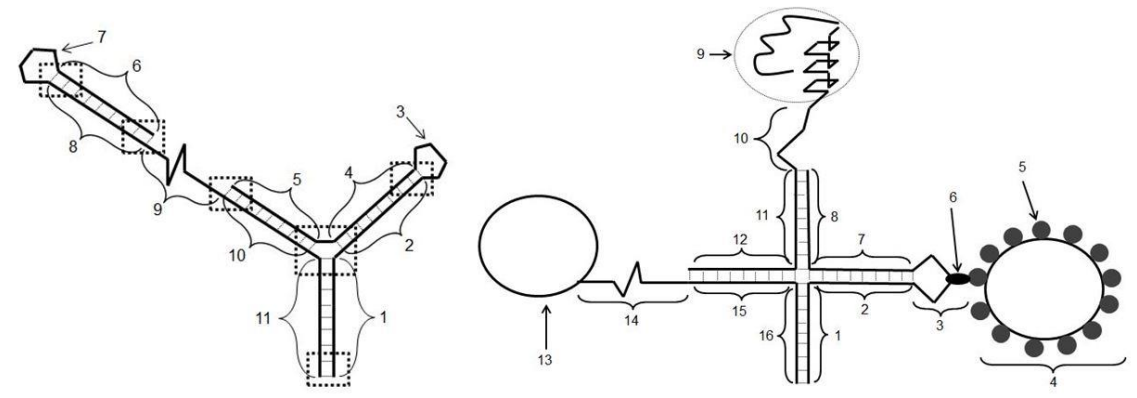


Figure 12. Left: Y-transducer for annealing-detection for presence of specified viral digests. The boxed regions indicate favorable areas for LNA substitution to protect the molecule in those regions from base-pair fraying at the terminus, loop-opening, or nexus-branchings. Right: A 4-way transducer (a.k.a, a Holliday Junction transducer). For dual aptamer/antibody tissue-targeting functional aptamer delivery studies, among other things, where a modulatory transducer is enabled by laser-tweezer coupling [42].

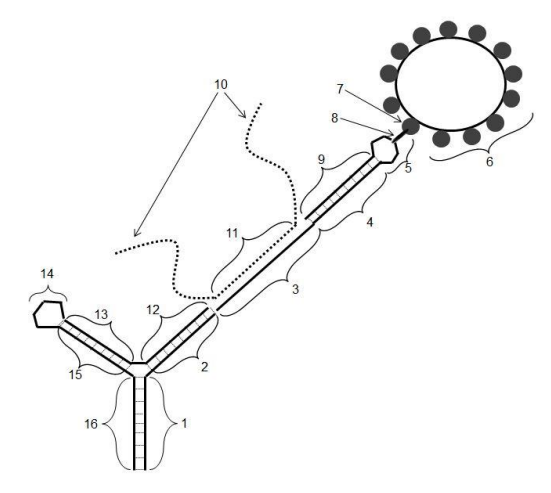


Figure 13. Y-transducer for single molecule annealing studies using twist mode modulations. Region 10 indicates the single stranded nucleic acid study molecule of interest: a nucleic acid whose region 10 section is annealed to region 3 of the transducer; where a magnetic bead is attached for laser-tweezer modulation (region 6), where the transducer is designed with sufficient LNA substitutions to allow laser-tweezer excitations to be transmitted as a twist-mode impulse through the annealed-target region. A twist mode will only transmit if the annealing-target is bound, giving rise to very different channel modulation signals. Paired regions {1,16}, {2,12},{4,9},{13,15} are designed to anneal with the dominant conformation shown, and are typically a minimum of 8 or 9 base-pairs in length. The loop in Region 14 is designed to not favor channel capture and strongly favor a single conformation for the Region 13-15 stem-loop region. Reprinted with permission [11].

Therapeutic use of aptamer methods, such as indicated in Fig 12, & 13 have begun to get FDA approval [33-37] in two settings: (1) dialysis therapy where aptamer-based filters are used to clean a patient's blood of accumulated kidney or liver toxins that are not being cleared due to damage to those organs; and (2) tissue or tumor directed treatments where the aptamer is linked to an antibody already known to target and localize to the tissue or tumor of interest.

5.3 Glycosylation assays and viral nucleic acid assays (further details in [42])

Two important application areas that have not been discussed are NTD-based glycosylation assays [38-40] and viral nucleic acid content (in blood-sample) assaying. Regarding the former, the nanopore detector can't easily see (via direct blockading interaction) roughly half of the protein surface modifications that have unfavorable charge (positive or neutral around pH 8 or 9), and any other modifications that may not be discernible via channel blockade due to unfavorable steric properties. In studies of neutral and positively charged polymers translocations with alpha-hemolysin channel [41] it is shown that an unfavorable charged molecule can be drawn into the channel. For the glycosylation profiling, however, there will often be negatively charged attachments much more highly favored for capture since the molecule will rotate to the most stable configuration, a configuration that happens to orient the more favorable charges for capture. The result is a strong bias towards the favorable charge groups present on an individual molecule. It may be possible to disrupt this orientation-bias on surface features by randomizing the molecular orientation prior to capture. An interference molecule like PEG could potentially be used for this purpose, but further discussion along these lines is outside the scope of this paper.

Thus, although albumin with pI 4.7 should be producing many blockade events, it has no glycosylations or other possible 'nanopore epitopes', so no blockades are seen from albumin even at high concentrations. When examining IgG antibodies, on the other hand, several distinctive, reproducible, signal classes occur, with possibly another dozen much rarer types of signal blockade. Antibodies are heavily glycosylated and glycated molecules, and the glycosylation profile of the Fc antibody region is critical in quality control for medicinal applications, so it appears that the nanopore offers a means to do glycosylation assays. A detailed antibody signal analysis is underway that is focused on antibody glycosylation assaying using direct measurements of channel modulations with a nanopore detector. In essence, isoelectric focusing gel information can be extracted not spatially along a gel track, but over time, according to a pH titration, and if urea is also introduced to strip away glycations, a direct glycation quantification can thereby be extracted via nanopore assaying. This experiment is outside the scope of this paper, so won't be discussed further (see [30]).

Regarding the viral nucleotide assaying there are two problems that will only briefly be discussed here, one problem has to do with obtaining the trace viral nucleotide sequences from a patient's blood sample and directly (no-PCR) perform

an annealing-based detection process. For this a polyethylene glycol (PEG) effective concentrator method can be employed that favors delivery of larger charged nucleic acids to the channel over proteins [1, 31]. In previous work a 'PEG-shift' nanopore/computational analysis was suggested for performing size-exclusion chromatography by such means [1, 38]. The other problem has to do with albumin and other lipid-bilayer intercalating molecules that may be present in large amounts in a blood sample. As mentioned, albumin doesn't pose a problem for the channel, but it can pose a problem for the bilayer in which the channel resides. In recent work a simple blood additive, PEG linked to albumin, appears to provide a membrane protective surface scaffolding [39, 40]. In practice, an albumin capture matrix could be used to prevent the normally high levels of blood albumin (the main protein in blood plasma) from entering the nanopore detector in the first place. Either way, the membrane shielding and nucleic acid concentrator experiment is outside the scope of this paper and won't be discussed further.

Whether considering air or water biosensing the mass production ease of aptamers is another significant advantage over mAb-based procedures. What is missing, however, is a mass discovery and refinement mechanism, where one possible solution involving the NTD is described in [1], where a variant of the NADIR SELEX procedure is used that introduces aptamers that are multifunctional, refining the specificity and affinity for a particular molecule or molecular feature, as with a standard aptamer, with a possible second binding function via aptamer or antibody, and having for another function the channel-current modulatory properties of a nanopore transduction reporter molecule that allows the binding properties of the binding moiety or moieties part to be directly assayed via the nanopore transduction detector (NTD) method.

In some settings, with large molecular features, large cell-surface features, or heavy metal chelation binding, more complex aptamer transducers, linked double-aptamer constructs, and dual aptamer/antibody binding moieties, all with nanopore modulator components, are indicated. The latter two arrangements are trifunctional in that they have two binding moieties and a nanopore modulatory component, for which NADIR augmented SELEX is even more advantageous. If a fourth functionality is introduced to receive laser-tweezer tugging, by linking a magnetic bead, then quadfunctional modulators are sought, strongly favoring the more directed tuning allowed with the nanopore detector.

6 Conclusions

A method is needed for inexpensive assaying of isomer mixtures that provides not only the ability to specifically bind a particular isomer with high affinity, but a means to multiplex profile a mixture of isomers with high accuracy. A nanopore transduction detector could be used to address this problem, where an aptamer or monoclonal antibody selected for the specific isomer binding of interest is linked to a uniquely modulating NTD transducer for direct quantification via the relative abundances of the different isomers-transducers observed at the nanopore. The nanopore device itself is quite inexpensive (the cost of the key components, including

patch clamp amplifier, comes to less than \$20,000). So the main cost barrier to NTD applications has been an easy (non-expert) and inexpensive procedure for designing and obtaining transducer molecules for binding interactions of interest. It is shown in this paper, however, that inexpensive assaying can be done with commoditized ('mail-order') components, such as from DNA labeling procedures, biotinylation procedures, and streptavidin-coating procedures (further details on transducer design in [42]). The transducer order-on-demand design process is made possible due to two results shown in this paper: (1) the complexity of transducer blockade modes appears to be limited to the orientation-toggling configuration-twisting semi-rigid-body motions of the dsDNA transducer molecule, which allows SCW signal processing to be performed in a manageable context. And, (2) laser-tweezer excitations can be used to drive transducers with magnetic bead attachments to arrive at high success-rate transducer designs. Regarding the latter, a general method for nanopore transduction detection transducer construction based on LNA/DNA chimeras that have twist-mode dominated state tracking for large charge/mass biomolecular complexes with long duplex DNA tether constructions is proposed, as is configuration-switching dominated state tracking for small charge/mass biomolecule complexes with short-linkage constructions.

The general-use nanopore transduction detector system offers the prospect for high-specificity molecular, molecular feature, and particulate testing (whether air-quality and water-quality testing), not only in the lab setting, but also the field setting (portable nanopore-based DNA sequencing devices are already commercially available, e.g., Oxford Nanopore Technologies). High-specificity detection is possible by incorporating the high binding specificity of aptamers and monoclonal antibodies for their binding targets into a nanopore binding-event transduction system. Once a binding event is transduced to an electrical ionic current flow measurement, novel channel current cheminformatics and machine learning methods are introduced for event classification. A quantification of the amount of bound versus unbound reporter molecule detected at the nanopore transduction detector then allows the concentration of the target molecule or particulate to be determined. A general procedure thus results for inexpensive LNA/DNA transducers to be obtained, where inexpensive low-power laser tweezer excitations can be used to retain the modulatory role of the transducer in its various states.

Acknowledgements. The author would like to thank META LOGOS Inc., for research support and a research license. (META LOGOS was co-founded by SWH in 2009.) The author would also like to thank the Meta Logos nanopore technicians Eric Morales and Joshua Morrison, and nanopore technicians Amanda Alba and Andrew Duda at the SWH Lab at The Research Institute for Children, Children's Hospital, New Orleans, for help gathering some of the data shown.

References

- [1] S. Winters-Hilt, Machine-Learning Based Sequence Analysis, Bioinformatics & Nanopore Transduction Detection, Lulu Publication, 2011.
- [2] S. Winters-Hilt, E. Horton-Chao, E. Morales, The NTD Nanoscope: potential applications and implementations, *BMC Bioinformatics*, **12** (2011), S10: S21. https://doi.org/10.1186/1471-2105-12-s10-s21
- [3] K. Thomson, I. Amin, E. Morales, S. Winters-Hilt, Preliminary nanopore cheminformatics analysis of aptamer-target binding strength, *BMC Bioinformatics*, **8** (2007), no. S7, S11. https://doi.org/10.1186/1471-2105-8-s7-s11
- [4] Stephen Winters-Hilt, The α-Hemolysin nanopore transduction detector single-molecule binding studies and immunological screening of antibodies and aptamers, *BMC Bioinformatics*, **8** (2007), no. S7, S9. https://doi.org/10.1186/1471-2105-8-s7-s9
- [5] A.M. Eren, I. Amin, A. Alba, E. Morales, A. Stoyanov and S. Winters-Hilt, Pattern Recognition Informed Feedback for Nanopore Detector Cheminformatics, Chapter in *Advances in Experimental Medicine and Biology*, Vol. 680, 2010, 99-108. https://doi.org/10.1007/978-1-4419-5913-3_12
- [6] Stephen Winters-Hilt, Amanda Davis, Iftekhar Amin and Eric Morales, Nanopore current transduction analysis of protein binding to non-terminal and terminal DNA regions: analysis of transcription factor binding, retroviral DNA terminus dynamics, and retroviral integrase-DNA binding, *BMC Bioinformatics*, **8** (2007), no. S7, S10. https://doi.org/10.1186/1471-2105-8-s7-s10
- [7] S. Winters-Hilt, Nanopore Detector based analysis of single-molecule conformational kinetics and binding interactions, *BMC Bioinformatics*, 7 (2006), no. S2, S21. https://doi.org/10.1186/1471-2105-7-s2-s21
- [8] S. Winters-Hilt, A. Stoyanov, Nanopore Event-Transduction Signal Stabilization for Wide pH Range under Extreme Chaotrope Conditions, *Molecules*, 21 (2016), no. 3, 346. https://doi.org/10.3390/molecules21030346
- [9] C. Tuerk, L. Gold, Systematic evolution of ligands by exponential enrichment: RNA ligands to bacteriophage T4 DNA polymerase, *Science*, **249** (1990), 505–510. https://doi.org/10.1126/science.2200121

- [10] S. Winters-Hilt, E. Morales, I. Amin, A. Stoyanov, Nanopore-based kinetics analysis of individual antibody-channel and antibody antigen interactions, *BMC Bioinformatics*, **8** (2007), no. Suppl 7, S20. https://doi.org/10.1186/1471-2105-8-s7-s20
- [11] S. Winters-Hilt, Biological system analysis using a nanopore transduction detector: from miRNA validation, to virus monitoring, to gene circuit feedback studies, *Advanced Studies in Medical Sciences*, **5** (2017), 13-53. https://doi.org/10.12988/asms.2017.722
- [12] M. Jain, I.T. Fiddes, K.H. Miga, H. Olsen, B. Paten, M. Akeson, Improved data analysis for the MinION nanoipore sequencer, *Nature Methods*, **12** (2015), 351-356. https://doi.org/10.1038/nmeth.3290
- [13] J. Schreiber, Z.L. Wescoe, R. Abu-Shumays, J.T. Vivian, B. Baatar, K. Karplus and M. Akeson, Error rates for nanopore discrimination among cytosine, methylcytosine, and hydroxymethylcytosine along individual DNA strands, *Proceedings of the National Academy of Sciences*, **110** (2013), no. 47, 18910-18915. https://doi.org/10.1073/pnas.1310615110
- [14] Y-L. Ying, J. Zhang, R. Gao, Y-T. Long, Nanopore-based sequencing and detection of nucleic acids, *Angewandte Chemie International Edition*, **52** (2013), no. 50, 13154-13161. https://doi.org/10.1002/anie.201303529
- [15] J.J. Kasianowicz, E. Brandin, D. Branton, D. W. Deamer. Characterization of individual polynucleotide molecules using a membrane channel, *Proc. Natl. Acad. Sci.*, 93 (1996), 13770-13773. https://doi.org/10.1073/pnas.93.24.13770
- [16] A. Meller, L. Nivon and D. Branton, Voltage-driven DNA translocations through a nanopore, *Phys. Rev. Lett.*, **86** (2001), no. 15, 3435-3438. https://doi.org/10.1103/physrevlett.86.3435
- [17] A. Meller, L. Nivon, E. Brandin, J. Golovchenko and D. Branton, Rapid nanopore discrimination between single polynucleotide molecules, *Proc. Natl. Acad. Sci.*, **97** (2000), no. 3, 1079-1084. https://doi.org/10.1073/pnas.97.3.1079
- [18] L. Kullman, M. Winterhalter and S. M. Bezrukov, Transport of Maltodextrins through Maltoporin: A Single-Channel Study, *Biophysical Journal*, 82 (2002), 803-812. https://doi.org/10.1016/s0006-3495(02)75442-8

- [19] L. Movileanu, S. Howorka, O. Braha, H. Bayley, Detecting protein analytes that modulate transmembrane movement of a polymer chain within a single protein pore, *Nat. Biotechnol.*, **18** (2000), 1091–1095.
- [20] Y. Astier, D. E. Kainov, H. Bayley, R. Tuma, S. Howorka, Stochastic detection of motor protein-RNA complexes by single-channel current recording, *ChemPhysChem*, 8 (2007), 2189–2194. https://doi.org/10.1002/cphc.200700179
- [21] S. Howorka, S. Cheley and H. Bayley, Sequence-specific detection of individual DNA strands using engineered nanopores, *Nat. Biotechnol.*, 19 (2001), no. 7, 636–639. https://doi.org/10.1038/90236
- [22] J. Li, D. Stein, C. McMullan, D. Branton, M.J. Aziz, J.A. Golovchenko, Ion-beam sculpting at nanometre length scales, *Nature*, **412** (2001), 166-169. https://doi.org/10.1038/35084037
- [23] C. Plesa, D. Verschueren, S. Pud, J. van der Torre, J.W. Ruitenberg, M.J. Witteveen, M.P. Jonsson, A.Y. Grosberg, Y. Rabin, C. Dekker, Direct observation of DNA knots using a solid-state nanopore, *Nat. Nanotechnol.*, 11 (2016), 1093-1097. https://doi.org/10.1038/nnano.2016.153
- [24] U.F. Keyser, J. van der Does, C. Dekker, N.H. Dekker, Inserting and manipulating DNA in a nanopore with optical tweezers, *Methods Mol. Biol.*, **544** (2009), 95-112. https://doi.org/10.1007/978-1-59745-483-4_8
- [25] R.M. Smeets, U.F. Keyser, N.H. Dekker, C. Dekker, Noise in solid-state Nanopores, *Proc. Natl. Acad. Sci.*, **105** (2008), no. 2, 417-421. https://doi.org/10.1073/pnas.0705349105
- [26] S. Carson, J. Wilson, A. Aksimentiev, M. Wanunu, Smooth DNA transport through a narrowed pore geometry, *Biophysical Journal*, **107** (2014), 2381-2393. https://doi.org/10.1016/j.bpj.2014.10.017
- [27] S. Carson, M. Wanunu, Challenges in DNA motion control and sequence readout using nanopore devices, *Nanotechnology*, **26** (2015), 074004. https://doi.org/10.1088/0957-4484/26/7/074004
- [28] M. Pastoriza-Gallego, G. Oukhaled, J. Mathe, B. Thiebot, J.-M. Betton, L. Auvray, J. Pelta, Urea denaturation of alpha-hemolysin pore inserted in planar lipid bilayer detected by single nanopore recording: loss of structural asymmetry, *FEBS Lett.*, **581** (2007), 3371-3376. https://doi.org/10.1016/j.febslet.2007.06.036

- [29] S. Winters-Hilt, Exploring protein conformation-binding relationships and antibody glyco-profiles using a nanopore transduction detector, *Mol. And Med. Chem.*, **2** (2016), e1378.
- [30] S. Winters-Hilt, Glyco-profiling a monoclonal antibody using a nanoscope. In preparation.
- [31] S. Winters-Hilt, W. Vercoutere, V. S. DeGuzman, D. Deamer, M. Akeson, and D. Haussler, Highly Accurate Classification of Watson-Crick Base-Pairs on Termini of Single DNA Molecules, *Biophys. J.* **84** (2003), 967-976. https://doi.org/10.1016/s0006-3495(03)74913-3
- [32] W. Vercoutere, S. Winters-Hilt, H. Olsen, D. Deamer, D. Haussler and M. Akeson, "Rapid Discrimination Among Individual DNA Molecules at Single Nucleotide Resolution Using an Ion Channel, *Nature Biotechnology*, **19** (2001), 248-252. https://doi.org/10.1038/85696
- [33] Dongxi Xiang, Sarah Shigdar, Greg Qiao, Tao Wang, Abbas Z. Kouzani, Shu-Feng Zhou, Lingxue Kong, Yong Li, Chunwen Pu and Wei Duan, Nucleic Acid Aptamer-Guided Cancer Therapeutics and Diagnostics: the Next Generation of Cancer Medicine, *Theranostics*, **5** (2015), no. 1, 23-42 https://doi.org/10.7150/thno.10202
- [34] Katherine Germer, Marissa Leonard, Xiaoting Zhang, RNA aptamers and their therapeutic and diagnostic applications, *Int. J. Biochem. Mol. Biol.*, **4** (2013), no. 1, 27-40.
- [35] Xin Ming, Brian Laing, Bioconjugates for targeted delivery of therapeutic oligonucleotides, *Advanced Drug Delivery Reviews*, **87** (2015), 81-89. https://doi.org/10.1016/j.addr.2015.02.002
- [36] Cindy Meyer, Ulrich Hahn and Andrea Rentmeister, Cell-Specific Aptamers as Emerging Therapeutics, *J. Nucl. Acids*, **2011** (2011), 904750. https://doi.org/10.4061/2011/904750
- [37] Ji Won Lee, Hyun Jung Kim & Kyun Heo, Therapeutic aptamers: developmental potential as anticancer drugs, *BMB Reports*, **48** (2015), no. 4, 234-237. https://doi.org/10.5483/bmbrep.2015.48.4.277
- [38] S. M. Bezrukov, I. Vodyanoy, R. A. Brutyan, J. J. Kasianowicz, Dynamics and free energy of polymers partitioning into a nanoscale pore, American Physical Society, Annual March Meeting, March 17-21, 1997, abstract #D41.10.

- [39] C. Makena Hightower, Beatriz Y. Salazar Va'zquez, Seetharama A. Acharya, Shankar Subramaniam, Marcos Intaglietta, PEG-Albumin Plasma Expansion Increases Expression of MCP-1 Evidencing Increased Circulatory Wall Shear Stress: An Experimental Study, *PLoS One*, **7** (2012), no. 6, e39111. https://doi.org/10.1371/journal.pone.0039111
- [40] Ragheb A. Assaly, Mustafa Azizi, David J. Kennedy, Cristine Amauro, Aiman Zaher, Frederick W. Houts, Robert H. Habib, Joseph I. Shapiro and J. David Dignam, Plasma expansion by polyethylene-glycol-modified albumin, *Clinical Science*, **107** (2004), 263–272. https://doi.org/10.1042/cs20040001
- [41] L. Movileanu, S. Cheley and H. Bayley, Partitioning of Individual Flexible Polymers into a nanoscopic protein pore, *Biophys. Journal*, **85** (2003), no. 2, 897-910. https://doi.org/10.1016/s0006-3495(03)74529-9
- [42] S. Winters-Hilt, Nanopore transducer engineering and design, Paper in preparation.

Supplement

S.1 Controlling Nanopore Noise Sources and Choice of Aperture [1]

The accessible detector bandwidth is delimited by noise resulting from 1/f (flicker) noise, Johnson noise, Shot noise, and membrane capacitance noise. For experimental operation at 1.0 M KCl at 23C, the α-hemolysin channel conducts 120 pA under an applied potential of 120 mV. The thermal noise contribution at the 1 GΩ channel resistance has an RMS noise current of 0.4 pA. During nanopore operation with 120pA current (with 10KHz bandwidth) there is, similarly, about 0.6 pA noise due to the discreteness of the charge flow. As with Johnson noise, the Shot noise spectrum is white. The specific capacitance of lipid bilayers is approximately 0.8 μF/cm² (very large due to molecular dimensions), and the specific conductance is approximately $10^{-6} \Omega^{-1} \text{cm}^{-2}$. In order for bilayer conductance to produce less RMS noise current than fundamental noise sources (under the conditions above). the leakage current must be a fraction of a pA. This problem is solved by reducing to less than a 500µm² bilayer area, for which less than 0.6 pA leakage current results and for which total bilayer capacitance is at most 4pF. This indicates that a decrease in bilayer area by another magnitude is about as far as this type of noise reduction can go. Preliminary attempts to do this, however, lead to a very unpredictable toxin intercalation rate, among other difficulties. For the experiments considered here, the aperture ranges in size between 20 microns in diameter and 25 microns in diameter (where smaller apertures are typically used in the single channel experiments and larger apertures in multi-channel experiments).

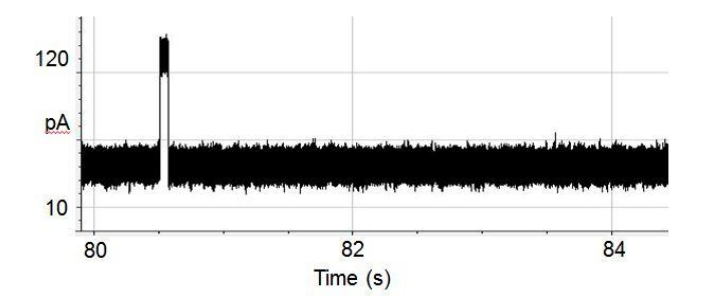
S.2 Signal Processing Methods [1]

With completion of FSA preprocessing, an HMM is used to remove noise from the acquired signals, and to extract features from them. The HMM configuration used

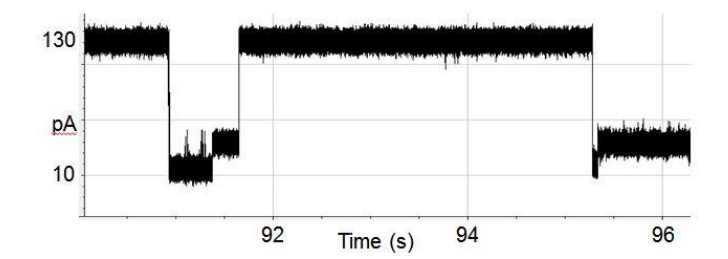
for control probe validation is implemented with fifty states that correspond to current blockades in 1% increments ranging from 20% residual current to 69% residual current [1,31]. In this HMM application the HMM states, numbered 0 to 49, corresponded to the 50 different current blockade levels in the sequences that are processed. The standard "grayscale" HMM, or 'generic HMM', feature extraction setup is then done: the state emission parameters of the HMM are initially set so that the state j, $0 \le j \le 49$ corresponding to level L = j+20, can emit all possible levels, with the probability distribution over emitted levels set to a discretized Gaussian with mean L and unit variance. All transitions between states are possible, and initially are equally likely. Each blockade signature is de-noised by 5 rounds of Expectation-Maximization (EM) training on the parameters of the HMM. After the EM iterations, 150 parameters are extracted from the HMM. The 150 feature vectors obtained from the 50- state HMM-EM/Viterbi implementation are: the 50 dwell percentage in the different blockade levels (from the Viterbi trace-back states), the 50 variances of the emission probability distributions associated with the different states, and the 50 merged transition probabilities from the primary and secondary blockade occupation levels (fits to two-state dominant modulatory blockade signals). Variations on the HMM 50 state implementation are made as necessary to encompass the signal classes under study.

The 150-component feature vector extracted for each blockade signal is then classified using a trained Support Vector Machine (SVM). The SVM training is done off-line using data acquired with only one type of molecule present for the training data (bag learning). Further details on the SVM and overall channel current cheminformatics signal processing are detailed in [1, 31].

S.3 20-bp DNA hairpin experiments for molecules 9GC-ext and 9GC-ext-mag [11]



Suppl. Figure 1. 9GC-ext with Faraday cage in place [11]. The brief upper level is the open channel baseline current level (at 121pA). The blockade commencing after the baseline lasted for 50sec, of which the first ~4s is shown. The 'fixed' blockade level is at 40pA.



Suppl. Figure 2. A less common, short duration, full-length 9GC-ext-mag blockade signal is shown [11] (before diffusional escape) with the beginning of another at far right. The Faraday cage is in-place for this trace, and the 42pA level is seen as before as the upper level toggle (but is less noisy than before since the cage in place). Two clear levels of blockade can be seen, and are thought to correlate with two distinct molecule-channel blockade configurations as usual. The toggle signals are thought to describe a switching between molecular loop/stem 'twist' states, however, and not between two channel blockade configurations (where the molecule in the same internal conformation).

S.4 Isomer resolution and chelator design

One of the most challenging problems imaginable for a molecular analyzer is to differentiate isomers when there are, literally, hundreds of isomers. Using NTD reporter/transducers that are developed to specifically bind to only one isomer, a more refined assay can be developed. Since the task is inherently multiplexed by the hundred or so different isomer targets that require quantification, it is important to not only be able to identify the bound/unbound state of the different isomer transducers, but to tell the different transducers apart from one another if simultaneously assayed in a mixture. Mixtures of DNA hairpins that differ only in their terminal base-pairs have been resolved with 99.9% accuracy [31], so the capability to engineer the bases of the Y-transducers such that they can be easily discriminated has been around for more than a decade. What is proposed here is a mixture of isomer Y-transducers, differing in their aptamer or antibody targeting arms, and in their associated Y-base terminus blockade signal, to arrive at an inexpensive process for multiplex isomer profiling. Since aptamers can be created in large quantities they have already become popular for use in biomarker discovery, similar procedures can be used here for novel isomer discovery using aptamers as well. Further details on transducer design are given in [42].

Received: March 5, 2017; Published: April 20, 2017